

FLUID COUPLED METALLIC MICROMACHINED NEEDLE ARRAYS

John Brazzle¹, Ian Papautsky², and A. Bruno Frazier^{1,2}

Departments of ¹Electrical Engineering and ²Bioengineering
50 S. Central Campus Dr., Rm. 2480, University of Utah, Salt Lake City, UT 84112
Tel: (801) 581-8611 Fax: (801) 585-5361 E-mail: brazzle@eng.utah.edu

ABSTRACT

In this paper, fluid coupled metallic micromachined needle arrays are designed, fabricated, and characterized. The described hollow metallic needle arrays include design features such as dual structural supports and needle coupling channels. The supports and needle walls are formed by micro-electroformed metal to provide increased structural integrity. The needle coupling channels are used to fluidically interconnect the needles and allow pressure equalization and balance of fluid flow between needles. In addition, the needle coupling channels minimize the effects of restricted needle passages by providing a redistribution point for fluid flow between them. The optimum design for the needle coupling channels is investigated using an ANSYS finite element numerical model. The significance of this work includes the development of hollow, metallic micromachined needle arrays for biomedical applications, as well as, a discussion of structural, fluidic, and biological design considerations.

INTRODUCTION

Micro instrumentation is a rapidly growing area of interest for a broad spectrum of engineering applications. One particularly fast growing area is biomedical instrumentation where significant efforts worldwide are made to develop micro biochemical analysis systems, physiological systems, and drug delivery systems [1,2]. A variety of manufacturing technologies are used to fabricate these micro systems, many of which are categorized under the set of technologies known as micromachining.

The number of biomedical applications for micromachining technologies is rapidly growing. Since micromachining technologies are relatively new, there is an increasing set of manufacturing techniques and critical applications still to be addressed. One application of interest to the biomedical industry is the development of microneedles. Some of the smallest hollow needles that are available today have inner diameters of over 400 μ m. To date, only microneedle arrays made of solid, non-hollow silicon have been realized [3]. It is clear that a demand exists for a needle device that can subcutaneously deliver medication

without the usual discomfort associated with current intravenous injection needles.

In order to determine the dimensions required for the conception of a microneedle that can penetrate the skin with a minimal amount of pain, an understanding of skin anatomy is required. Human skin is made of three layers: stratum corneum, viable epidermis, and dermis [4]. The outer 10-15 μ m of skin, called stratum corneum, is primarily made of dead tissue. The viable epidermis, 50-100 μ m below the stratum corneum, contains living cells, but is void of blood vessels and contains few nerves. Below the viable epidermis lies the dermis, which forms the bulk of the skin volume and contains nerves and blood vessels. This implies that a microneedle could be designed to be minimally invasive, in that, the needle would only penetrate just beyond the viable epidermis, reaching the capillaries and minimizing the chance of encountering and piercing the nerves present in the area of penetration.

This paper presents the design and fabrication of the fluid coupled micromachined needle array. Each array is composed of hollow metallic microneedles fabricated on top of a silicon substrate using micromachining surface fabrication techniques [5]. Every microneedle of the array consists of input shafts and cantilevered output shafts (Figure 1). A novel cross-flow design (needle coupling channels) is incorporated to equalize pressure distribution and minimize the effects of clogged passages within the needles. The

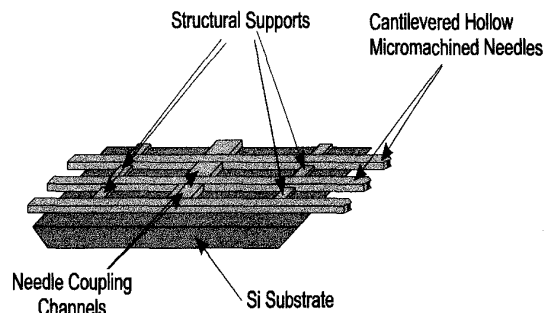


Figure 1. Schematic representation of the fluid coupled micromachined needle array.

optimum design for the needle coupling channels is investigated using an ANSYS finite element numerical model. The process used to fabricate the fluid coupled micromachined needle array includes p⁺ etch-stop membrane technology, anisotropic etching of silicon in potassium hydroxide, sacrificial thick photoresist micromolding technology, and micro-electrodeposition technology.

The number of needles in 2-D arrays can vary from 10's to 100's. The needle length extended from the substrate can be varied from below 50 μm (subcutaneous) to several millimeters for fluid delivery/extraction. The inner cross-sectional dimensions of individual needles range from 10 μm to 1 mm in width and 5 μm to 50 μm in height.

The fluid coupled micromachined needle arrays have many advantages, including: (a) reduced trauma at penetration site (small size), (b) greater freedom of patient movement (minimal penetration), (c) a practically pain-free drug delivery device (distribution of force), (d) precise control of penetration depth (needle extension length), and (e) can be stacked and packaged into a 3-D device for fluid transfer.

FLUID THEORY AND MODELING

Before the design and fabrication of the microneedles can be accomplished successfully, it is necessary to determine the validity of the design. This is obtained by developing the appropriate numerical model that accounts for microchannel dimensions, as well as, fluid flow characteristics.

The general equations that govern the motion for a viscous compressible fluid in Cartesian coordinates can be written as:

$$\mu \nabla^2 \mathbf{V} - \nabla p + \rho \mathbf{f} = \rho \dot{\mathbf{V}} \quad (1)$$

where a superimposed dot indicates a material derivative, \mathbf{V} is the fluid velocity vector, \mathbf{f} represents the external forces (e.g., gravity), μ is the fluid viscosity, and ∇p is the pressure gradient required to move the fluid [6]. These equations are generally known as the Navier-Stokes equations. For the case of a Newtonian fluid with constant physical properties (water) and negligible external forces (no effects of gravity) moving through a rectangular microchannel, the flow is two-dimensional and the Navier-Stokes equations can be further simplified to:

$$\frac{\partial^2 \mathbf{V}}{\partial x^2} + \frac{\partial^2 \mathbf{V}}{\partial y^2} - \frac{1}{\mu} \nabla p = 0 \quad (2)$$

where x is the direction along the microchannel width and y is the direction along the microchannel height.

These equations were solved numerically for flow of water through an array of 10 microneedles using commercially developed ANSYS software based on the finite element method. The needle channel dimensions used in the analysis are 40 μm wide and 2 mm long. The coupling channels between each needle channel are 100 μm wide. The

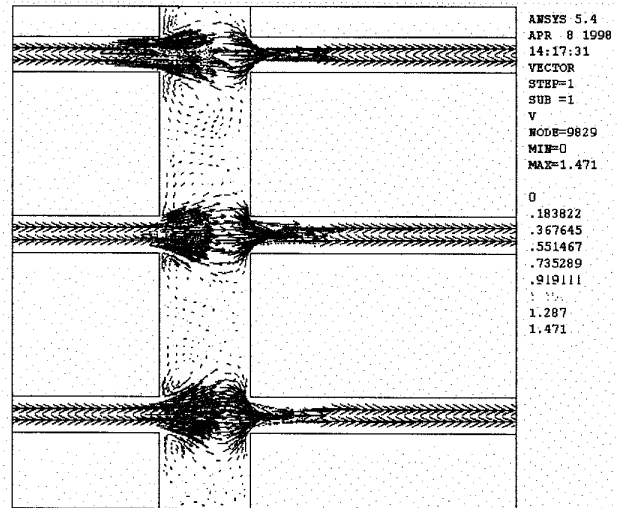


Figure 2. Vector magnitude plot showing a close-up view of the fluid velocity interaction in the needle coupling channels with no obstructions in the fluid path.

flow rate at the needle inputs was set to 1 cc/sec.

Figure 2 shows a vector magnitude plot illustrating the effects the needle coupling channels for unobstructed needle channels. The coupling channels appear to not interfere with the flow in the needle channels. The vectors in the center of each needle channel represent the greatest magnitude, while the small vectors in the center of each needle coupling channel signify a vector magnitude of zero.

The characteristics of the fluid flow and the effect of the coupling channels were analyzed for the case of fully restricted needle channels (Figure 3). The flow in the needle channel with a fully restricted input is augmented by the incoming fluid flow from the other needle channels by means

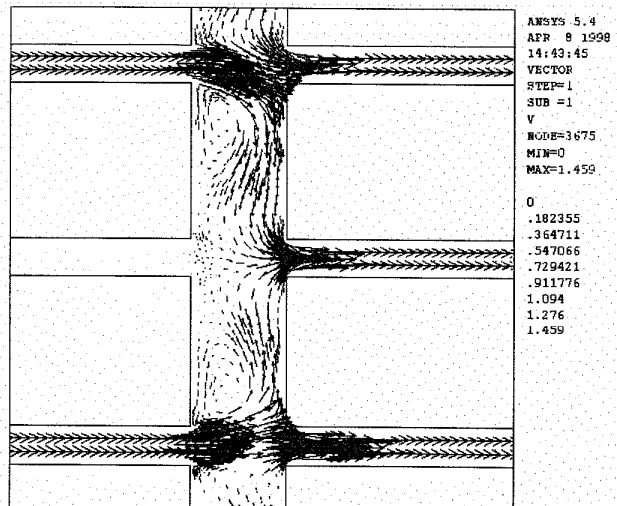


Figure 3. Plot of vector magnitude showing fluid velocity interactions within the needle coupling channels for the case of a fully restricted input needle channel (center).

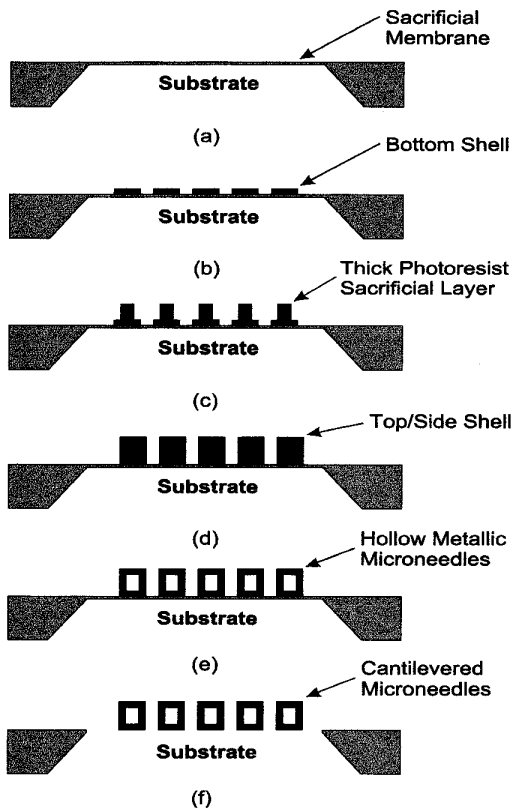


Figure 4. Needle array fabrication procedure: (a) Create silicon membrane using high temperature p⁺ doping and KOH etching; (b) electroplate bottom shell; (c) apply and pattern thick photoresist; (d) deposit metal forming side walls and top shell; (e) remove thick photoresist using acetone bath; (f) release micro needles by plasma etching the p⁺ membrane.

of the needle coupling channels. In the event that a clog is encountered in one of the output needle channels, the result is similar, with the exception that the flow from the input needle channel is redistributed to the unclogged channels (Figure 6).

The needle coupling channels, as depicted in the ANSYS numerical model, were fortuitous at redistributing the fluid flow as necessary when needle inputs or outputs were obstructed. Therefore, the dimensions of the needles and coupling channels used in the analysis are practical for implementation into the design and fabrication of the fluid coupled micromachined needle arrays.

FABRICATION

The fluid coupled metallic micromachined needle arrays are fabricated using both newly developed and established micromachining technologies [5]. Initially, one side of a silicon wafer is heavily doped with boron using high temperature thermal diffusion to form a 3-5 μm p⁺ layer. Silicon nitride (Si_3N_4) is deposited on both sides of the wafer using plasma-enhanced chemical vapor deposition (PECVD)

and is used as a mask during the subsequent anisotropic etching of silicon in 20% KOH [7]. The p⁺ boron layer serves as an etch stop, resulting in a thin sacrificial membrane upon which the length of the metallic needles are fabricated and subsequently released (Figure 4a). Next, a metal system of adhesion layers and an electroplating seed layer are electron beam evaporated onto the insulating Si_3N_4 film. Using standard photolithography techniques, this metal layer is patterned and 20 μm of palladium is electroplated to form the bottom wall of the microneedle (Figure 4b) [8]. The use of palladium as a structural material provides high mechanical strength and durability, as well as, biocompatibility for use in biomedical applications [9].

Next, 20 μm of commercially available thick photoresist is deposited and patterned into sacrificial structures (Figure 4c). An 800 \AA seed layer of gold is sputter deposited onto the photoresist structures. A 20 μm layer of palladium is electroplated forming the sidewalls and the top of the microneedles (Figure 4d). The sacrificial thick photoresist is then removed using acetone, producing the hollow metallic microneedles (Figure 4e). In the final step, the sacrificial p⁺ membrane is removed by reactive ion etching in SF_6 plasma. Thus, the microneedle ends are released from the sacrificial membrane and are freely suspended, projecting outward from the silicon substrate (Figure 4f).

RESULTS

Individual needles of the 2-D arrays fabricated to date have an inner cross-sectional area of 40 \times 20 μm^2 (W \times H) with outer dimensions of 80 \times 60 μm^2 . A micromachined needle array fabricated on silicon and released from its substrate is shown in Figure 10. The needle coupling channels are positioned at the center of each needle and are 100 μm wide. Two sets of 60 \times 100 μm^2 structural supports are 250 μm from each needle end. The needle wall thickness

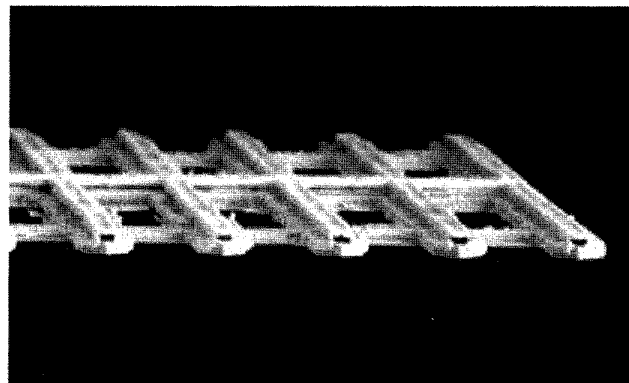


Figure 5. SEM of micromachined needle array. Individual needle channels are 2 mm long and have center-to-center spacing of 200 μm . The inner dimensions are approximately 20 \times 40 μm^2 . The total needle array width is 5.2 mm. Needle coupling channels are centered along the length of each needle and are 100 μm wide.

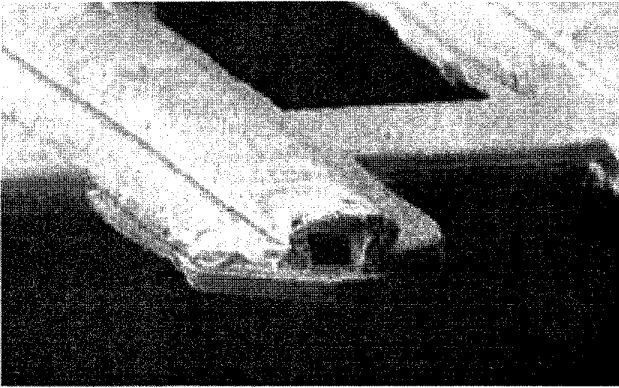


Figure 6. SEM of a micromachined microneedle output tip. The inner dimensions are approximately $30 \times 20 \mu\text{m}^2$, while the outer dimensions are approximately $80 \times 60 \mu\text{m}^2$.

is approximately $20 \mu\text{m}$ of electroformed palladium. Each needle channel is 2 mm long, while the total width of the 25-needle array is 5.2 mm . The center-to-center spacing of individual needles is $200 \mu\text{m}$.

It is especially important to note the quality of the fabrication of the tip of each needle, since this is the part that will be inserted through skin for drug delivery. Figure 6 is a SEM showing a close-up of one of the needle tips. The inner dimensions are approximately $30 \times 20 \mu\text{m}^2$, while the outer dimensions are approximately $80 \times 60 \mu\text{m}^2$. The distance from the needle tip to the structural supports is $250 \mu\text{m}$. The needle tip is formed by a 45° angle for ease of penetration.

Flows in channels of similar dimensions have been experimentally examined [10]. Experimental data, shown in Figure 7, is in close agreement with the predictions of the Navier-Stokes theory and the model based on the micropolar fluid theory.

CONCLUSION

Micromachined needle arrays have been designed, fabricated, and characterized. The design includes arrays of 25 needles with fluid coupling channels and dual structural supports. Numerical modeling of the fluid flow characteristics was performed, demonstrating that the needle coupling channels redistribute flow when the input or output ports are fully restricted. Micromachining technologies have been used to batch fabricate hollow metallic fluid coupled needle arrays. The significance of this work includes the development of the hollow metallic micromachined needle arrays for biomedical applications, as well as, a discussion of structural, fluidic, and biological design considerations. The micromachined needle array has many advantages, including (a) reduced trauma at penetration site (small size), (b) greater freedom of patient movement (minimal penetration), (c) a practically pain-free drug delivery device (distribution of force), (d) precise control of penetration depth (needle

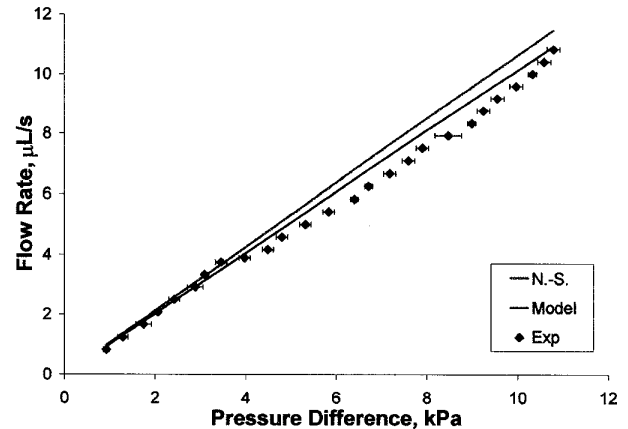


Figure 7. Comparison of experimental data with the Navier-Stokes theory and a model based on the micropolar fluid theory for water flow in microchannels ($3000 \times 600 \times 30 \mu\text{m}^3$, $L \times W \times H$) [10].

extension length), and (e) can be stacked and packaged into a 3-D device for fluid transfer.

ACKNOWLEDGMENTS

The author would like to acknowledge the University of Utah Undergraduate Research Opportunities Program (UROP), Lucent Technologies (Bell Labs) for their palladium bath chemistry, and Hoechst Inc. for supplying thick photoresist.

REFERENCES

- [1] B.K. Gale, A.B. Frazier, and K. Caldwell, *MEMS 97*, Nagoya, Japan, Jan. 26-30, 1997.
- [2] P. Rai-Choudhury, Ed. *Microlithography, Micromachining, and Microfabrication: Volume 2*, SPIE Press, Bellingham, Washington, 1997.
- [3] S. Henry, D.V. McAllister, M.G. Allen, and M.R. Prausnitz, *MEMS 98*, Heidelberg, Germany, Jan. 25-29, 1998.
- [4] R.H. Champion, J.L. Burton, and F.J.G. Ebling, Eds. *Textbook of Dermatology*, Blackwell Scientific: London, 1992.
- [5] I. Papautsky, J. Brazzle, H. Swerdlow, and A.B. Frazier, *J. Microelectromech. Sys.*, in press.
- [6] V. N. Constantinescu, *Laminar Viscous Flow*. Springer, NY 1995.
- [7] H. Siedel, L. Csepregi, and A. Heuberger, *J. Electrochem. Soc.*, vol. 37, 1990, pp. 3612-3620.
- [8] I. Kadija, V. Chinchankar, V.T. Eckert, E.J. Kudrak, J. Alys, *Proc. of the 77th Annual Conference of the American Electroplaters and Surface Finishers Society*, July, 1990.
- [9] J. Black, *Biological performance of materials: Fundamentals of biocompatibility*, Marcel Dekker, New York, 1992.
- [10] I. Papautsky, J. Brazzle, T. Ameel, and A. B. Frazier, *MEMS 98*, Heidelberg, Germany, Jan. 25-29, 1998.